

Electronic Supplementary Information

A novel strategy for the design of smart supramolecular gels: control the stimuli-response properties through competitive coordination of two different metal ions

Qi Lin,* Bin Sun, ‡ Qing-Ping Yang, ‡ Yong-Peng Fu, Xin Zhu, Tai-Bao Wei and
You-Ming Zhang*

*Key Laboratory of Eco-Environment-Related Polymer Materials, Ministry of Education of China, Key
Laboratory of Polymer Materials of Gansu Province, College of Chemistry and Chemical Engineering,
Northwest Normal University, Lanzhou, Gansu, 730070, P. R. China.*

Table of Contents

Materials and instruments

Synthesis of gelator **G**

Scheme S1. The synthetic route to organogelator **G**.

Characterization of **G**

Scheme S2. Chemical structure of the **G** and the presumed self-assembly and stimuli-responsive mechanism.

Table S1. Gelation Property of Organogelator **G**.

Fig. S1 (a) Plots of critical gelation concentrations (CGCs) of **G** in the different solvents. (b) Plots of T_{gel} against the concentrations of organogel **OG** and metallo gels **CaG** and **CaFeG** in ethanol

Fig. S2 Photographs of organogel of **G** in ethanol (1% w/v) and organogels of **G** in the presence of various metal ions

Fig. S3 Fluorescence spectra of organogel of **G** (**OG**) in ethanol (1% w/v) and organogels of **G** in the presence of various metal ions.

Fig. S4 Fluorescence spectra of organogel **OG**, metallo gels **CaG**, **FeG** and **CaFeG**

Fig. S5 Temperature-dependent fluorescent spectra of the **CaG** during gelation process.

Fig. S6 Fluorescence spectra of **CaFeG** with increasing concentration of $H_2PO_4^-$

Fig. S7 Partial 1H NMR spectra of **G** in $CDCl_3$ with different concentrations and partial 1H NMR spectra of **G** mixed with 1 equiv. of Ca^{2+} in $CDCl_3$.

Fig. S8 FT-IR spectra of powdered **G** and xerogel of organogel **OG**

Fig. S9 FT-IR spectra of powdered **G** and xerogel of metallo gel **CaG** and **CaFeG**

Fig. S10 SEM images of xerogel of **OG**, **CaG**, **CaFeG** and **CaFeG** xerogel treated with $H_2PO_4^-$ in situ.

Fig. S11 Powder XRD patterns of xerogel of **OG**, **CaG**, **CaFeG** and **CaFeG** xerogel treated with $H_2PO_4^-$

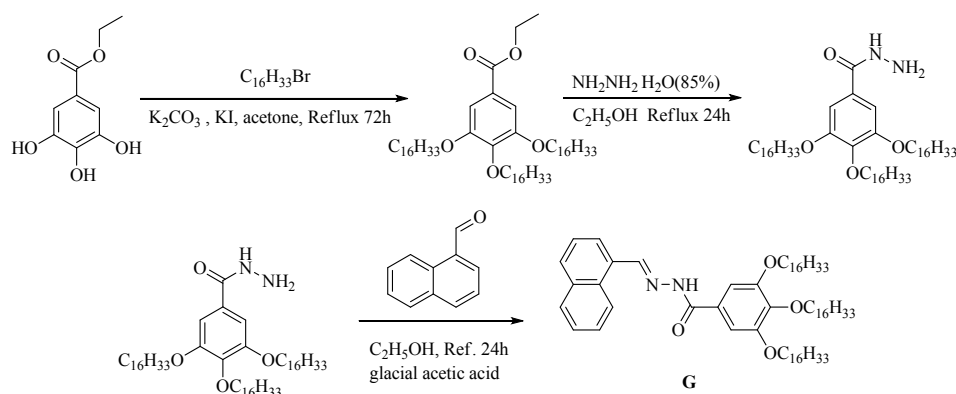
Materials and instruments

All reagents and starting materials were obtained from commercial suppliers and used as received unless otherwise noted. All anions were used as sodium salts while all cations were used as the perchlorate salts, which were purchased from Alfa Aesar and used as received. Fresh double distilled water was used throughout the experiment. Nuclear magnetic resonance (NMR) spectra were recorded on Varian Mercury 400 and Varian Inova 600 instruments. Mass spectra were recorded on a Bruker Esquire 6000 MS instrument. The X-ray diffraction analysis (XRD) was performed in a transmission mode with a Rigaku RINT2000 diffractometer equipped with graphite monochromated CuK α radiation ($\lambda = 1.54073 \text{ \AA}$). The morphologies and sizes of the xerogels were characterized using field emission scanning electron microscopy (FE-SEM, JSM-6701F) at an accelerating voltage of 8 kV. The infrared spectra were performed on a Digilab FTS-3000 Fourier transform-infrared spectrophotometer. Melting points were measured on an X-4 digital melting-point apparatus (uncorrected). Fluorescence spectra were recorded on a Shimadzu RF-5301PC spectrofluorophotometer. Elemental analyses were performed by Thermo Scientific Flash 2000 organic elemental analyzer.

Synthesis of gelator G

Compounds 3,4,5-tris(hexadecyloxy)benzo-hydrazide were synthesized according to literatures methods.¹ **G** was synthesized as follow: 1-naphthaldehyde (1 mmol), 3,4,5-tris(hexadecyloxy)benzohydrazide (1 mmol) and acetic acid (0.1 mL, as a catalyst) were added to ethanol (20 mL). Then the reaction mixture was stirred under

refluxed conditions for 24 hours, after removing the solvent, yielding the precipitate of **G**. Recrystallized with CHCl₃-C₂H₅OH to get solid of **G**.

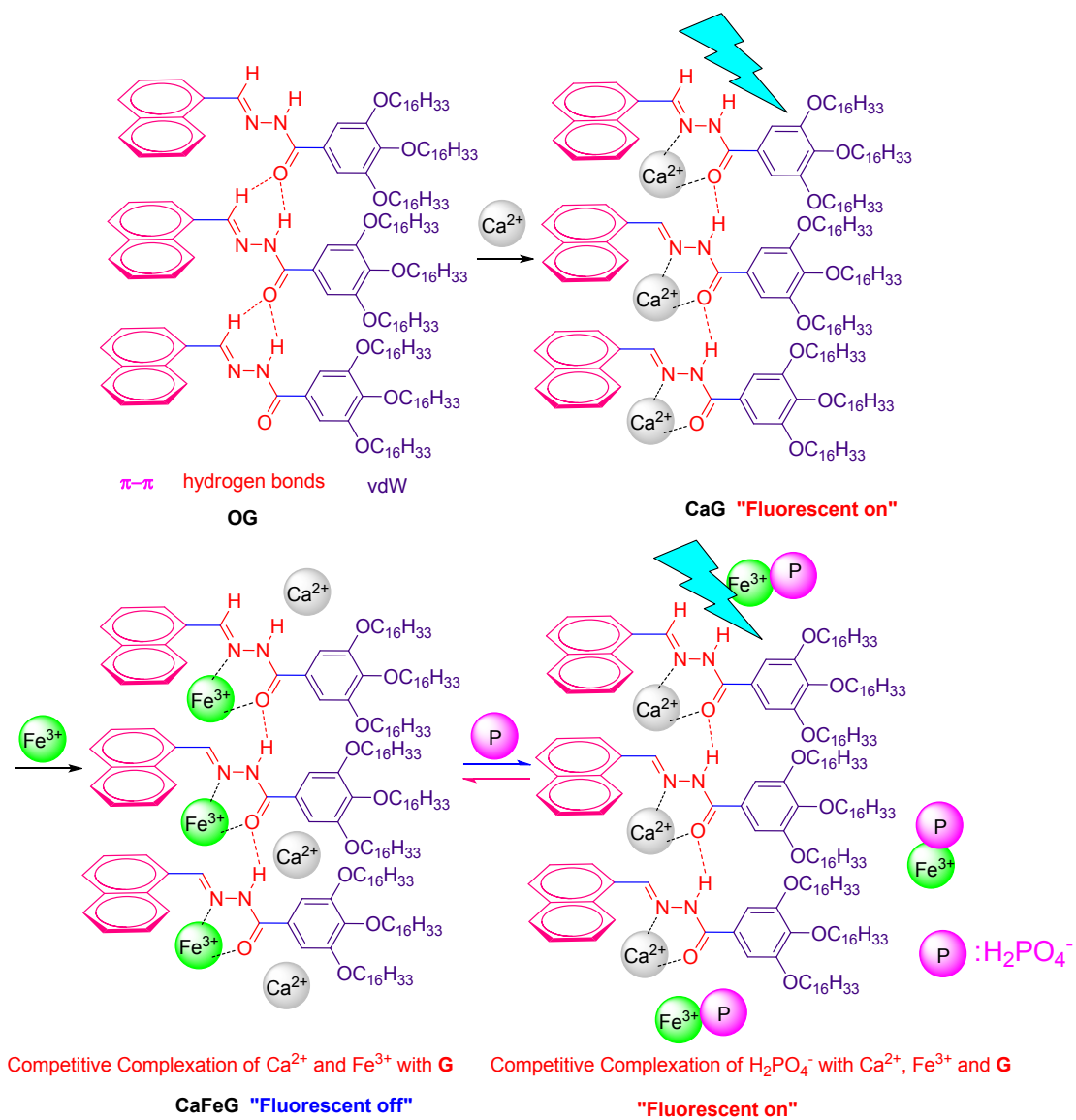


Scheme S1. The synthetic route to organogelator **G**.

Characterization of G: Yield: 75%, m.p. 89-91 °C ¹H NMR (CDCl₃, 400 MHz): δ, 9.77 (s, 1H, -NH), 9.04 (s, 1H, -N=CH), 8.85 (d, *J* = 6.4 Hz, 1H, -ArH), 7.99 (s, 1H, ArH), 7.87 (t, *J* = 7.8 Hz, 2H, -ArH), 7.51-7.45 (m, 3H, -ArH), 7.11 (s, 2H, -ArH), 3.98 (t, *J* = 6.4 Hz, 6H, -OCH₂), 1.77 (t, *J* = 6.9 Hz, 6H, -OCH₂CH₂), 1.43~1.25 (m, 72H, -CH₂), 0.88 (t, *J* = 6.2 Hz, 9H, -CH₃). ¹³C NMR (CDCl₃, 100 MHz): 166.95, 152.78, 142.26, 141.34, 107.87, 133.80, 131.10, 130.71, 129.06, 128.82, 127.74, 127.37, 127.00, 126.19, 125.26, 124.60, 107.87, 105.91, 105.12, 73.56, 73.45, 69.39, 69.11, 68.92, 31.93, 30.34, 30.23, 29.73, 29.67, 29.38, 29.28, 29.17, 26.09, 22.70, 14.13. IR (KBr, cm⁻¹) ν: 3450 (N-H), 1717(C=O), 1649 (C=N); MS-ESI calcd for C₆₆H₁₁₁N₂O₄ [**G** + H]⁺: 995.8544; found: 995.8096. Elemental analysis calcd for C₆₆H₁₁₀N₂O₄: C, 79.62; H, 11.14; N, 2.81; found: C, 79.51; H, 11.23; N, 2.69.

Reference:

1. Y.-P. Fu, Q. Lin, T.-B. Wei, P. Chen, X. Zhu, X. Liu, Y.-M. Zhang, *Chem. Reagents*, 2013, **35**, 367-368.



Scheme S2. The presumed self-assembly and stimuli-responsive mechanism of OG and metallogel.

Table S1 . Gelation Property of Organogelator **G**.

Entry	Solvent	State ^a	CGC ^b	$T_{\text{gel}}^{\text{c}}$ (°C, wt%)
1	Cyclohexane	S	\	\
2	Toluene	S	\	\
3	Petroleum ether	P	\	\
4	THF	S	\	\
5	Chloroform	S	\	\
6	Dichloromethane	F	\	\
7	Acetone	F	\	\
8	Acetonitrile	S	\	\
9	DMF	G	0.6	45(1%)
10	DMSO	P	\	\
11	Methanol	F	\	\
12	Ethanol	G	0.4	69(1%)
13	Ethenediol	F	\	\
14	Propyl alcohol	G	0.5	50(1%)
15	Isopropanol	F	\	\
16	<i>n</i> -Butyl alcohol	G	0.6	60(1%)
17	<i>n</i> -Amyl alcohol	PG	\	\
18	Isoamyl alcohol	G	0.8	52(1%)
19	Hexyl alcohol	PG	\	\

^a G, P, F, PG, and S denote gelation, precipitation, fluid, partial gelation and solution, respectively, c = 1%.

^b The critical gelation concentration (wt%, 10mg/mL = 1%).

^c The gelation temperature(°C).

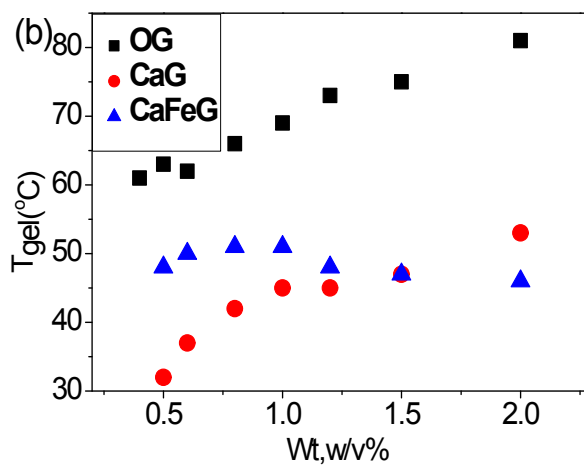
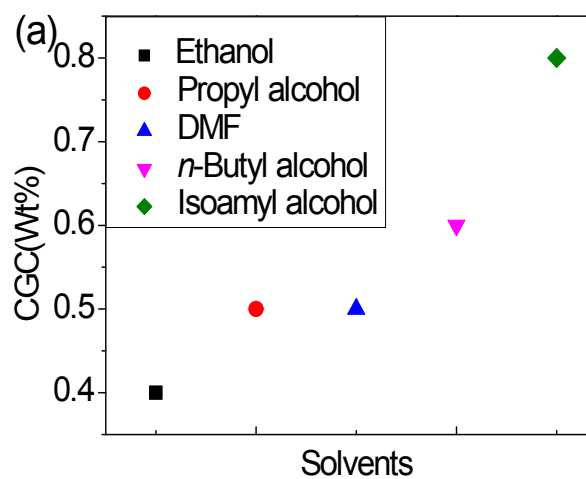


Fig. S1 (a) Plots of critical gelation concentrations (CGCs) of **G** in the different solvents. (b) Plots of T_{gel} against the concentrations of organogel **OG** and metallogels **CaG** and **CaFeG** in ethanol (for **CaG**, **G** : Ca^{2+} = 1 : 1; for **CaFeG**, **G** : Fe^{3+} : Ca^{2+} = 1 : 2 : 1).

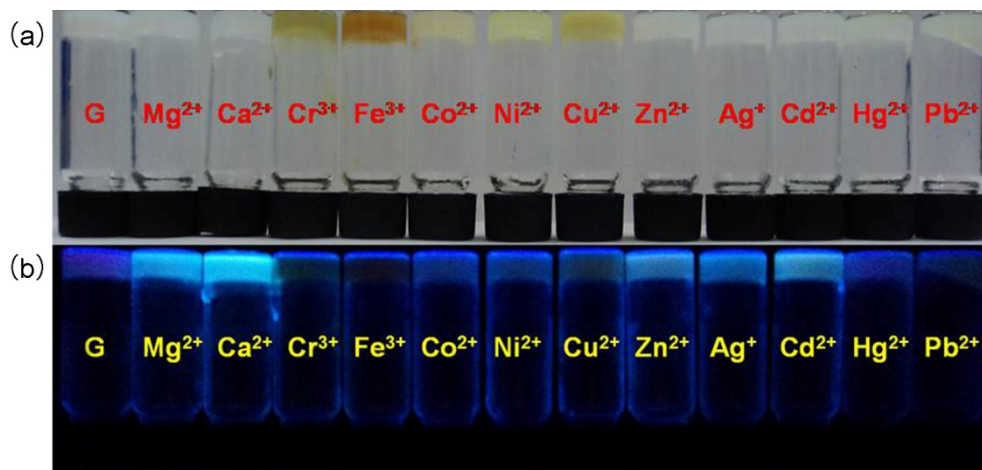


Fig.S2 Photographs of organogel of **G** in ethanol (1% w/v) and organogels of **G** in the presence of various metal ions (in ethanol, 1%, w/v, using their perchlorate salts as the sources, **G**: cation = 1 : 1) under (a) room (b) UV light.

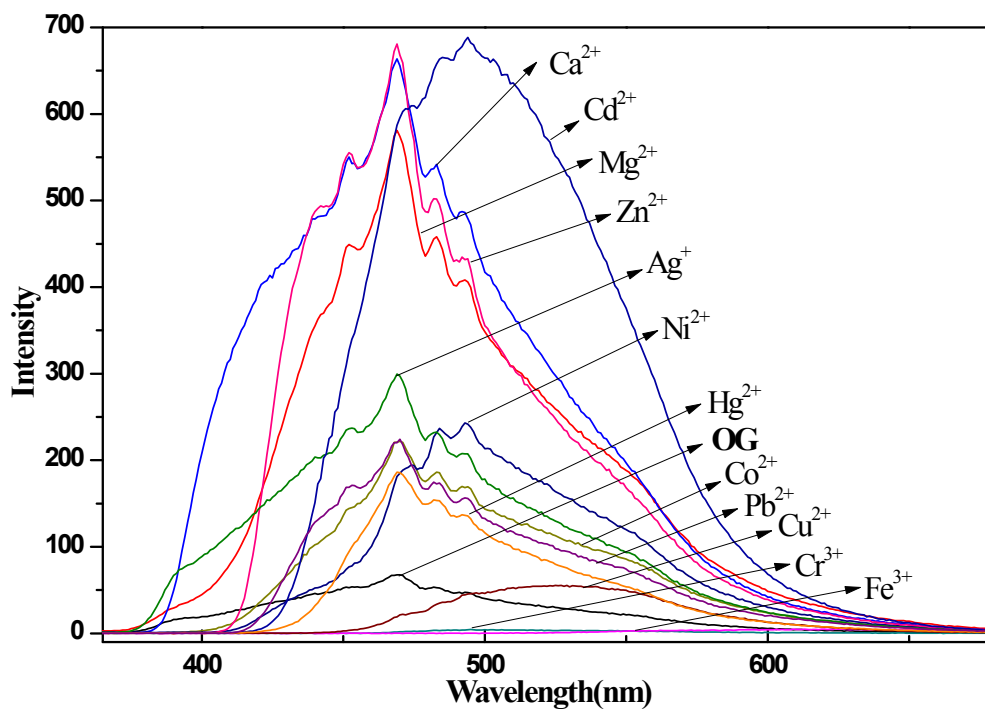


Fig.S3 Fluorescence spectra of organogel of **G** (**OG**) in ethanol (1%, w/v) and organogels of **G** in the presence of various metal ions (in ethanol, 1%, w/v, using their perchlorate salts as the sources, **G**: cation = 1 : 1, λ_{ex} = 350 nm).

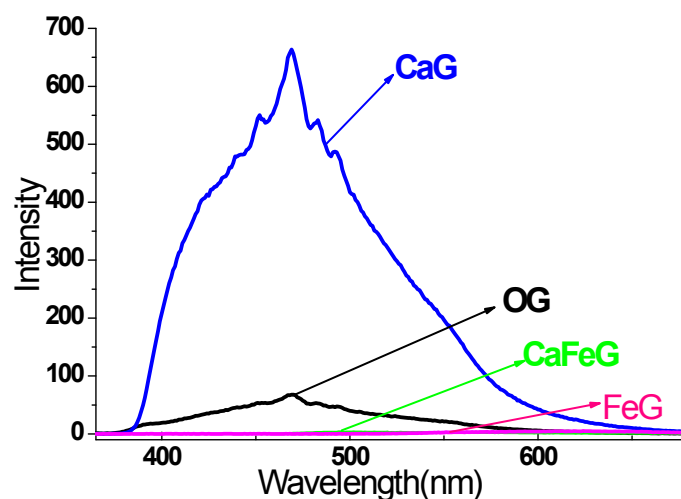


Fig. S4 Fluorescence spectra of organogel **OG** (1%, in ethanol), metallogels **CaG**, **FeG** and **CaFeG** (1%, in ethanol, for **CaG**, $G : Ca^{2+} = 1 : 1$; for **FeG**, $G : Fe^{3+} = 1 : 1$; for **CaFeG**, $G : Fe^{3+} : Ca^{2+} = 1 : 2 : 1$).

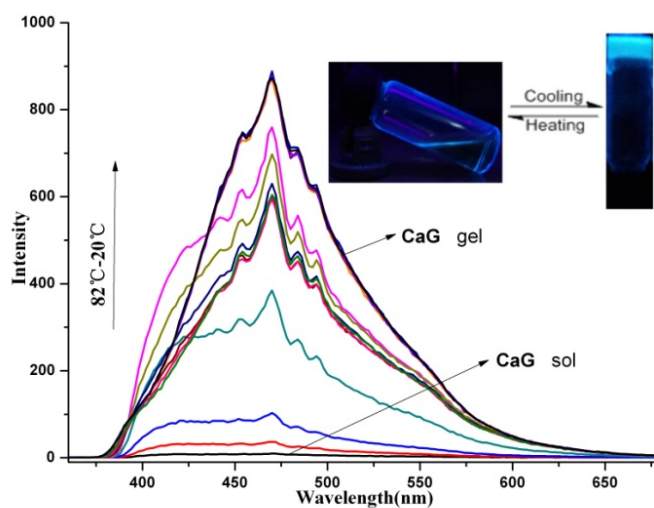


Fig. S5 Temperature-dependent fluorescent spectra of the **CaG** during gelation process.

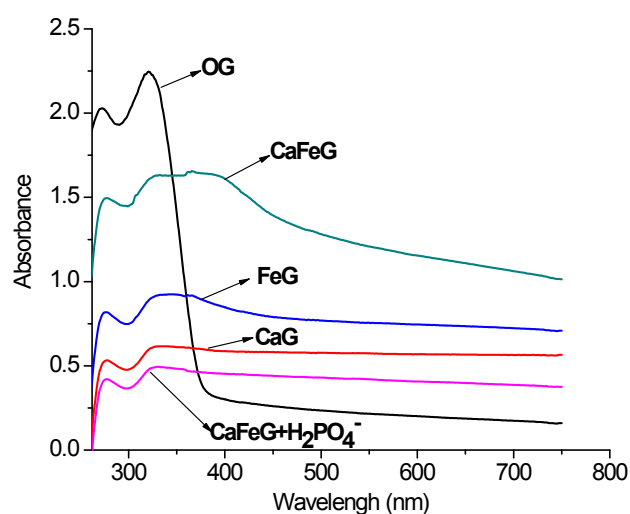


Fig. S6 UV-vis spectra of the xerogel films of **OG** (obtained from 1 % ethanol organogel); **CaG** (obtained from 1% ethanol metallogel, **CaG**, **G** : $\text{Ca}^{2+} = 1 : 1$); **CaFeG** (obtained from 1% ethanol metallogel, **CaFeG**, **G** : $\text{Fe}^{3+} : \text{Ca}^{2+} = 1 : 2 : 1$); **FeG** (obtained from 1% ethanol metallogel, **FeG**, **G** : $\text{Fe}^{3+} = 1 : 2$); **CaFeG** xerogel treated with H_2PO_4^- in situ.

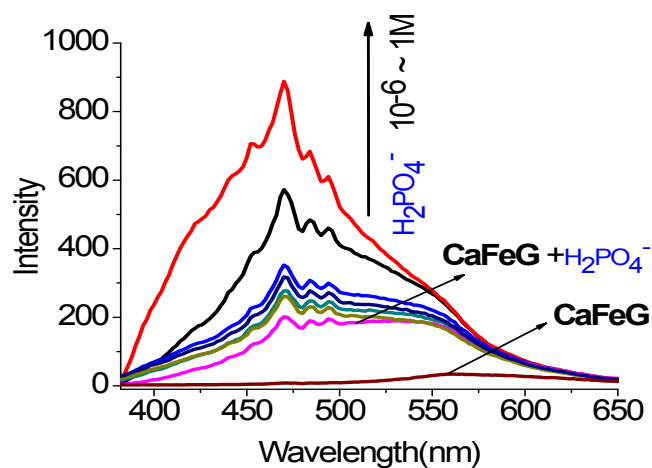


Fig. S7 Fluorescence spectra of **CaFeG** with increasing concentration of H_2PO_4^-

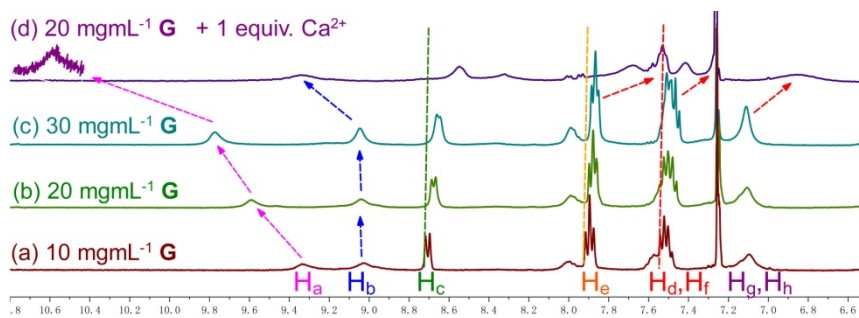


Fig. S8 (a-c) Partial ^1H NMR spectra of **G** in CDCl_3 with different concentrations. (d) Partial ^1H NMR spectra of **G** mixed with 1 equiv. of Ca^{2+} in CDCl_3 .

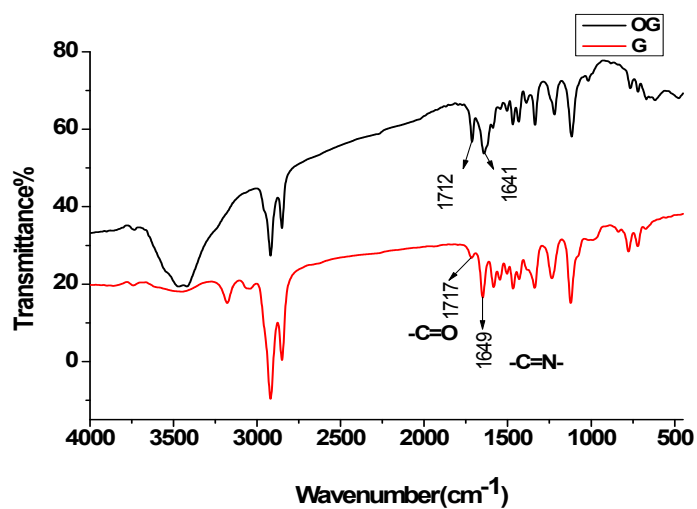


Fig. S9 FT-IR spectra of powdered **G** and xerogel of organogel **OG** (obtained from 1 % ethanol organogel).

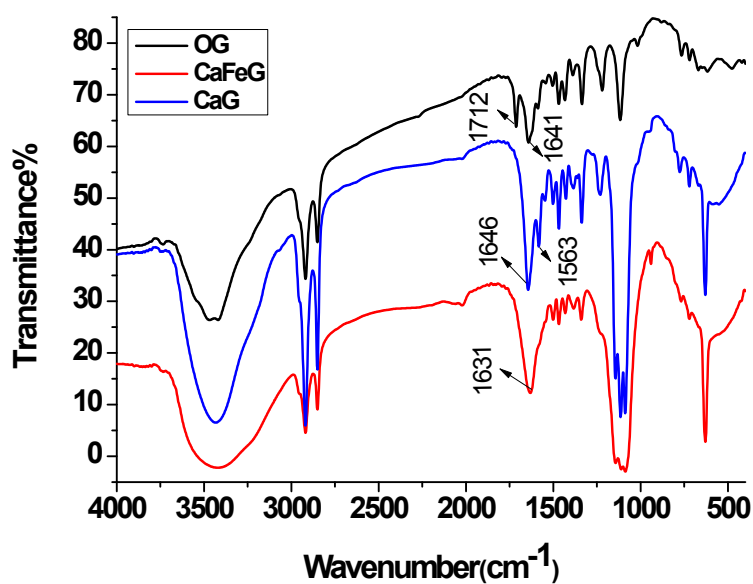


Fig. S10 FT-IR spectra of powdered **G** and xerogel of metalloel **CaG** (obtained from 1% ethanol metalloel, **CaG**, **G** : Ca^{2+} = 1 : 1) and **CaFeG** (obtained from 1% ethanol metalloel, **CaFeG**, **G** : Fe^{3+} : Ca^{2+} = 1 : 2 : 1).

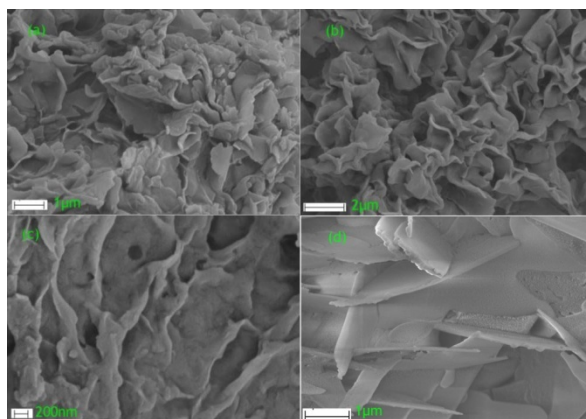


Fig. S11 SEM images of xerogel of (a) **OG** (obtained from 1 % ethanol organogel) (b) **CaG** (obtained from 1% ethanol metalloel, **CaG**, **G** : Ca^{2+} = 1 : 1) (c) **CaFeG** (obtained from 1% ethanol metalloel, **CaFeG**, **G** : Fe^{3+} : Ca^{2+} = 1 : 2 : 1); (d) **CaFeG** xerogel treated with H_2PO_4^- in situ.

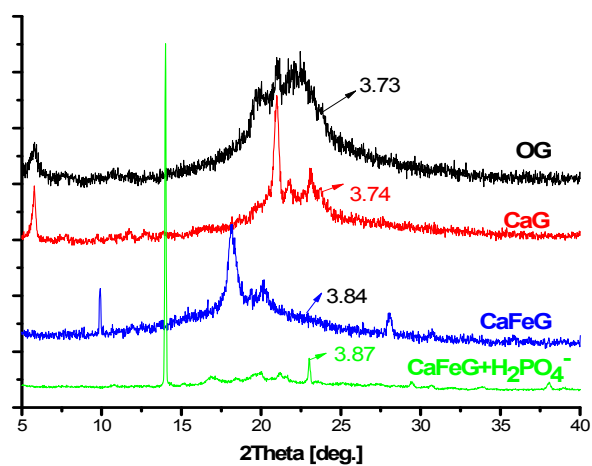


Fig. S12 Powder XRD patterns of xerogel of **OG** (obtained from 1 % ethanol organogel), **CaG**, **CaFeG** (obtained from 1% ethanol metallogel, for **CaG**, **G** : $\text{Ca}^{2+} = 1 : 1$; for **CaFeG**, **G** : $\text{Fe}^{3+} : \text{Ca}^{2+} = 1 : 2 : 1$) and **CaFeG** xerogel treated with H_2PO_4^- (5 equiv., using $0.1 \text{ mol L}^{-1} \text{ NaH}_2\text{PO}_4$ water solution as the H_2PO_4^- sources).